



**Jacobs University Bremen
Department of Physics and Earth Sciences**

**Molecular Dynamics Simulation of
Porphyrin Adsorption on Clay for the
formation of a Light Harvesting System**

BSc Thesis in Physics
as part of the course
CA08-200304 Thesis Physics

by

Carlos Rafael Salazar Letona

Bremen, May 17, 2021

Supervisor: Prof. Ulrich Kleinekathöfer
2nd Reader: Prof. Stefan Ketteman

Contents

1	Introduction	4
1.1	Molecular Dynamics Simulation	4
1.1.1	Molecular Interactions	4
1.1.2	The MD Algorithm	7
1.2	Dye-Sensitized Solar Cells	8
1.3	Light Harvesting System	10
2	Procedure	11
2.1	Topologies Preparation	11
2.2	Solvation	14
2.3	Ionization	14
2.4	Energy Minimization	15
2.5	NVT and NPT Equilibration	16
2.6	Generation of Initial Configuration	18
3	Results and Discussion	21
3.1	Determination of Inter-charge Distances	21
3.2	Porphyrin Movement through the Simulation	22
3.3	Assessing the Adsorption Percentage	26
3.4	Intermolecular Distance of Porphyrins	26
3.5	Relationship between Inter-charge Distances	28
4	Conclusion and Outlook	30
5	Acknowledgements	32
6	References	33

Abstract

In this thesis several simulations were performed with the objective of studying the adsorption of porphyrin molecules on a montmorillonite surface. The systems simulated consisted of sixteen porphyrins and a clay surface with different charge densities. In all of the cases some adsorption of the porphyrins on the surface was observed. The simulation was performed using the GROMACS software, results were visualized using VMD and analyzed using the MDanalysis library on python. The results of the simulation are in agreement with the expected configuration from other sources. The relation between the inter-charge distance in porphyrins and clay and the adsorption capabilities of the surface was proved. It was found that the adsorption has a peak in the area where the inter-charge distance difference is 0. A hypothesis could be formed on the reason for the decrease in adsorption when electric interactions are stronger, in which the interaction of the solvent and ions is stronger.

1 Introduction

1.1 Molecular Dynamics Simulation

Computer simulations are useful for the understanding of the properties of a system of molecules in terms of their structure and interaction between its components. The simulation technique utilized for this thesis was Molecular Dynamics. Through Molecular Dynamics (MD), the properties of a system like transport coefficients, responses to perturbations, etc. can be analyzed [1]. By using computer simulations, the macroscopic world of the laboratory can be connected to microscopic lengths and time scales. With it, an interpretation of the system and the interaction between molecules can be made, as accurate as our current computational power may allow us. It can also be used to study systems that are too difficult to produce in the laboratory. The aim of MD is not to have a perfectly realistic model, but to have one that contains the essential physics in order to compare to experiments.

1.1.1 Molecular Interactions

In MD, the atoms and molecules are allowed to interact for a certain time, in order to get a picture of the evolution of the system. In most of the implementations of MD the trajectories of atoms and molecules are calculated by numerically solving Newton's equations of motion. For a simple atomic system, they are written as

$$m_i \ddot{\mathbf{r}}_i = \mathbf{f}_i \quad \mathbf{f}_i = -\frac{\partial}{\partial \mathbf{r}_i} \mathcal{U} \quad (1)$$

In order to solve the equations we need to calculate the forces \mathbf{f}_i acting on the atoms, which are derived from the potential energy $\mathcal{U}(\mathbf{r}^N)$ as a function of the atomic coordinates $\mathbf{r}^N = (\mathbf{r}_1, \mathbf{r}_2, \dots, \mathbf{r}_N)$ representing the complete set of $3N$ atomic coordinates.

Potential energy has two main sources when it comes to interaction with other atoms, bonded and non-bonded interactions. The first one represents the interaction between atoms of the same molecules, the second one is the most computationally expensive, as it represents the interaction of an atom with the other atoms in the system.

Non-bonded interactions

The potential energy has a part $\mathcal{U}_{non-bonded}$ which represents the non-bonded interactions and is usually split into 1-body, 2-body, 3-body ... terms:

$$\mathcal{U}_{non-bonded}(\mathbf{r}^N) = \sum_i u(\mathbf{r}_i) + \sum_i \sum_{j>i} v(\mathbf{r}_i, \mathbf{r}_j) + \dots \quad (2)$$

The first term represents external potential fields or the effects of container walls. This term is usually ignored for fully periodic simulation boxes. In these simulations, container walls were used in the positive and negative z axis. The second term represents the 2-body interactions, and it is usually focused on

the most while higher order body interactions are neglected [2]. If all the pairwise electrostatic and van der Waals interactions were considered, then a MD simulation would scale by $\mathcal{O}(n^2)$.

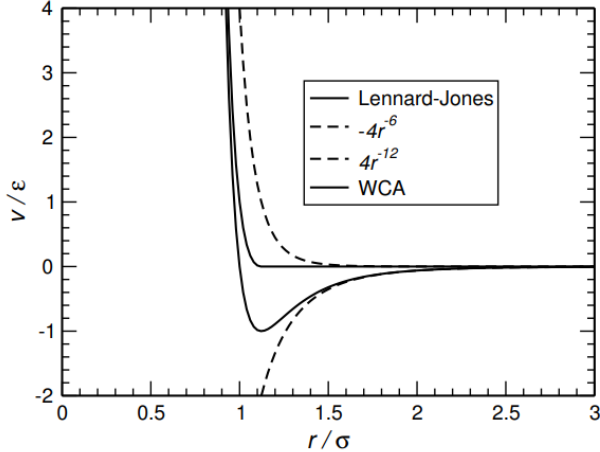


Figure 1: Lennard-Jones potential showing the contributions from r^{-12} and r^{-6} . Retrieved from [1]

For the non-bonded potential, Lennard-Jones potential is the most used form:

$$v^{LJ}(r) = 4\epsilon \left[\left(\frac{\sigma}{r}\right)^{12} - \left(\frac{\sigma}{r}\right)^6 \right] \quad (3)$$

where the parameters σ and ϵ represent the diameter and the depth of the well as shown in fig 1. In GROMACS these parameters are defined in the topology file for every type of atom [3]. In some applications the attractive interactions are of less concern than the volume effects which dictate molecular packing. In these cases the WCA model is used, shown also in fig 1, which consists on truncating the potential at the minimum and shifting it upwards.

If there are charges present, then the Coulomb potential is also considered:

$$v^{Coulomb}(r) = \frac{Q_1 Q_2}{4\pi\epsilon_0 r} \quad (4)$$

where Q_1 and Q_2 are the charges, and ϵ_0 is the permittivity of free space.

Bonded interactions

Molecules are built out of site-site potentials with a similar form to equation 3. Quantum-chemical calculations are usually carried out to get the electron density throughout the molecules. The intramolecular interactions are modelled in the simplest way by using:

$$\mathcal{U}_{intramolecular} = \frac{1}{2} \sum_{bonds} k_{ij}^r (r_{ij} - r_{eq})^2 \quad (5a)$$

$$+ \frac{1}{2} \sum_{\substack{bend \\ angles}} k_{ijk}^\theta (\theta_{ijk} - \theta_{eq})^2 \quad (5b)$$

$$+ \frac{1}{2} \sum_{\substack{torsion \\ angles}} \sum_m k_{ijkl}^{\Phi,m} (1 + \cos(m\Phi_{ijkl} - \gamma_m)) \quad (5c)$$

which depend on the separation, bend angle and torsion angle, described in fig 2. The **bonds** term is calculated using the separation between pairs of atoms. For this term a harmonic form is assumed using an equilibrium separation. The **bend angles** term is calculated using the θ_{ijk} angle between successive bond vectors, involving three atom coordinates as:

$$\cos \theta_{ijk} = \hat{\mathbf{r}}_{ij} \cdot \hat{\mathbf{r}}_{jk} = (\mathbf{r}_{ij} \cdot \mathbf{r}_{ij})^{-1/2} (\mathbf{r}_{jk} \cdot \mathbf{r}_{jk})^{-1/2} (\mathbf{r}_{ij} \cdot \mathbf{r}_{jk}) \quad (6)$$

This bending term is usually defined as quadratic in the displacement from equilibrium. The **torsion angles** term uses the angle Φ_{ijkl} which is defined in terms of three bonds, therefore four coordinates are considered:

$$\cos \Phi_{ijkl} = -\hat{\mathbf{n}}_{ijk} \cdot \hat{\mathbf{n}}_{jkl}, \quad \mathbf{n}_{ijk} = \mathbf{r}_{ij} \times \mathbf{r}_{jk}, \quad \mathbf{n}_{jkl} = \mathbf{r}_{jk} \times \mathbf{r}_{kl} \quad (7)$$

Where \mathbf{n} is the normal to the plane defined by each pair of bonds. Once the potential energy function is specified the next step is to calculate the forces by using equation 1.

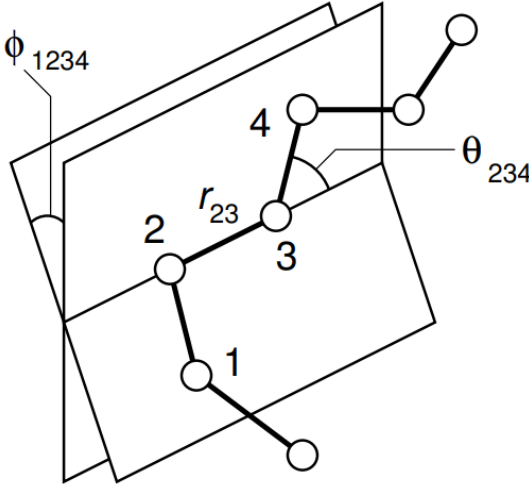


Figure 2: Scheme of simple chain molecule. Retrieved from [1]

1.1.2 The MD Algorithm

The equations used for Molecular Dynamics are nothing new, but the success of MD comes from the advancements in numerical algorithms. The classical equations of motion can be written using the momentum of the particle as a system of coupled ordinary differential equations:

$$\dot{\mathbf{r}}_i = \mathbf{p}_i/m_i \quad \text{and} \quad \dot{\mathbf{p}}_i = \mathbf{f}_i \quad (8)$$

For the simulations performed for this project the algorithm of Velocity Verlet was used. Verlet algorithms are commonly used in MD because they offer good numerical stability, time reversibility, etc. and it has a computational cost similar to the Euler method.

For a starting configuration that is out of equilibrium the forces may be excessively large, producing the MD simulation to fail. For this reason energy minimization is necessary in many cases. EM consists in determining the global minimum of the potential energy in a reasonable amount of time [3]. In GROMACS, energy minimization is implemented using the steepest descent method. This algorithm finds the minimum of the energy by using derivative information. The partial derivatives of the potential energy with respect to the coordinates is already known in MD programs, so this algorithm works as a modification of MD programs [3].

In order to keep systems and their simulations computationally feasible, small sample sizes are used. To compensate for the small size, periodic boundary conditions are used. This means that in order to avoid surface effects from

affecting the system, the system is surrounded with replicas of the system itself. The problem of atoms leaving the boundaries of the system is also solved with this, as they can be simply replaced with the image coming from the adjacent replica, as shown in fig 3. By getting rid of the artifact caused by unwanted boundaries, a new artifact is introduced, which is caused by the periodic conditions. If the system being simulated is crystalline, then periodicity might be something desired. In the simulations performed for this thesis, the periodic boundary conditions were desired in the x and y axis, as it would help to approximate larger surfaces. However, the periodic conditions on the z axis were turned off, as interaction with different clay sheets is undesired. This was done by setting atomic walls on the positive and negative z axis. This would also help simulate a larger surface area, as the height could be decreased without worrying about the periodic image of the surface.

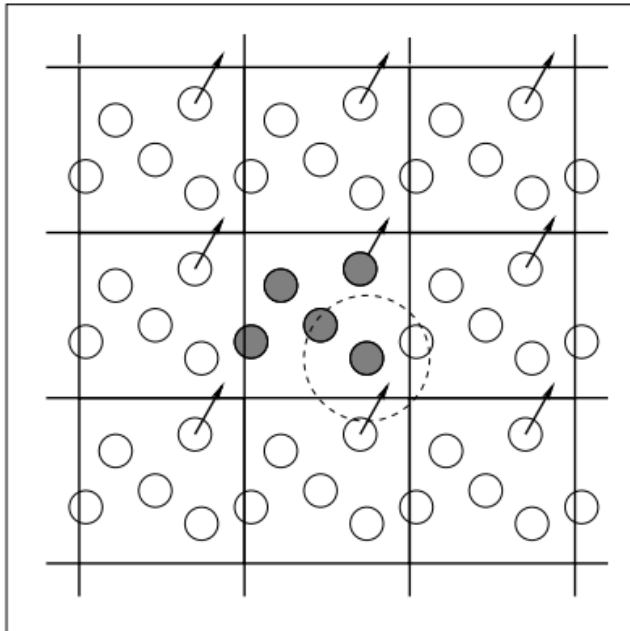


Figure 3: Periodic boundary conditions. As a particle leaves the simulation box, an image particle enters. Retrieved from [1]

1.2 Dye-Sensitized Solar Cells

Due to the ever more noticeable effects of the utilization of fossil fuels and the increase in population, it has become more imperative to find alternatives for energy production. There are many renewable energy alternatives, but their capabilities still not fully compare with fossil fuels, making it more difficult to have a complete transition. For this reason, more and more research is

being done on increasing the efficiency obtained from the different types of renewable energies. Solar energy is the most famous renewable energy, and it was considered to be promising for the future. However, the implementation of solar energy comes with many problems. There is an obvious issue with the temporal availability of solar energy, but there are more subtle but equally concerning problems. These subtle problems are related to the process and the materials used in their fabrication, as well as the availability of these materials.

Dye-sensitized solar cells (DSC) come as an alternative to typical solid-state junction solar cells. They stem from a third generation of cells, which offer the prospective of very low-cost fabrication [4]. DSCs are a prototype from this family of devices that performs the optical absorption, and the charge separation processes by the association of a sensitizer with a wide band gap semiconductor. They have become relevant in the last decades as they are an alternative to silicon-based solar cells by offering lower production costs and higher efficiencies [5].

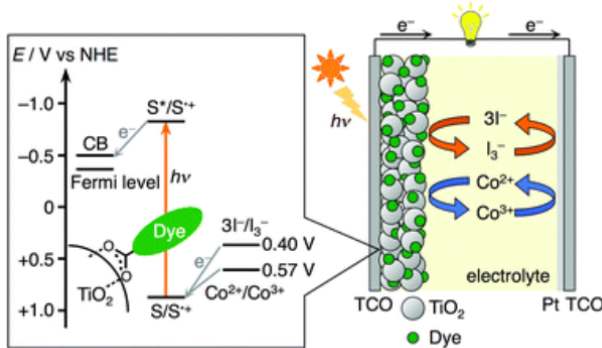


Figure 4: Components and operational principles of dye-sensitized solar cells. Retrieved from [5]

A scheme of a typical DSC can be seen in fig 4. It consists of a dye-sensitized photoanode, a platinum counter electrode and an electrolyte in between both which contains a redox mediator. The dyes in the photoanode adsorb photons and perform charge separation through photoinduced electron injection from the excited state of the dye into the conduction band of the semiconductor. The dyes that are now cations are then reduced by the redox electrolyte [6].

The efficiency of DSCs strongly depends on the type of sensitizer dye that is being used. Porphyrins have been a candidate for sensitizers since the beginning of DSCs. Porphyrins are being utilized in research because of their intense absorption bands in the visible region, flexible modifications of their core, and easy manipulation of the electronic structures [5].

1.3 Light Harvesting System

In nature, the arrangement of regular molecules can collect sunlight efficiently and carry the excitation energy smoothly to the reaction center. This arrangement of molecules forms what is called a light-harvesting system (LHS). A strategy to form one of these LHS is to construct a structure of regularly arranged dyes.

In order to create this structure a host material is needed. Clay minerals are an ideal option used for this purpose, as they are negatively charged surfaces that consist of nanostructured flat sheets with exfoliation or stack abilities, and they also have optical transparency in the visible region when exfoliated [7]. In this project Montmorillonite was used as a surface material, shown in fig 8. Montmorillonite was used as it possesses the same characteristics of having permanent negative charges, and it is already being studied for the adsorption of other substances [8].

For the dyes, Porphyrin molecules are used. Two types of porphyrins are used, m-TMPyP and p-TMPyP, and they are utilized in a 3:1 ratio. Two porphyrins are being used as it was shown that the absorption spectra of m-TMPyP/p-TMPyP complexes is identical to the sum of the individual adsorption of m-TMPyP and p-TMPyP [7]. The ratio used was chosen as it was proved that it is one of the ratios with the highest energy transfer efficiency [7]. The molecular structures of the porphyrins are shown in fig 5. The regular arrangement of this can form a LHS, with a very high energy transfer efficiency, as shown in fig 6. The expected final system is shown in fig 7.

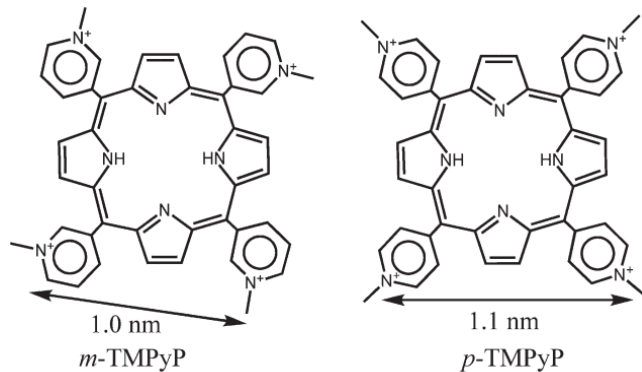


Figure 5: Porphyrin molecules used in the simulation. Retrieved from [7]

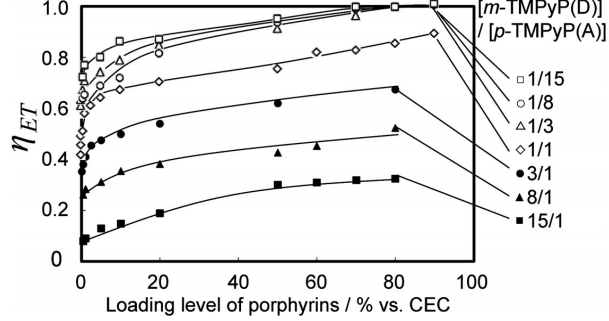


Figure 6: Energy transfer efficiency for different ratios of porphyrins. Retrieved from [7]

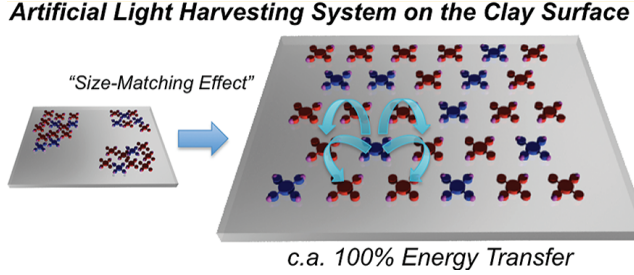


Figure 7: Clay/Porphyrin system arrangement. Retrieved from [7]

2 Procedure

The simulation made in this project consists in reproducing the formation of a Porphyrin/Clay system using GROMACS [3]. The system consists of a clay surface (Montmorillonite) and two types of porphyrins. For the porphyrins twelve molecules of p-TMPyP and four of m-TMPyP were used. The purpose of the simulation was to produce a system in which the porphyrins adhered to the clay surface, produced by the positive charge of the porphyrins and the negative charge of the surface.

2.1 Topologies Preparation

In order to perform the simulations, the topology files have to be obtained first. For this, the online tool of CHARMM-GUI [9] was utilized to produce the topology file of the Montmorillonite surface. This online tool allows for the customization of the surface. Under the nanomaterial modeler section of the input generator the material can be chosen. Then, box options are given to define the size of the surface. The ratio of defect and ion options can also be modified, which becomes an important quantity in the study of these simulations. The

chemical formula is the following:

$$(K, Na)_x[Si_4O_8][Al_{(2-x)}Mg_xO_2(OH_2)] \quad (9)$$

The ratio of defect and ion options consists of the x value shown in this Equation. The x-value has a range of $0 \leq x < 0.95$. By changing this value, the number of Al atoms in the surface is changed and they are substituted by Mg atoms, hence changing the charge of the surface. The periodic options are then selected for the x and y axis, as periodic conditions in the z axis are not of importance for these simulations. The system is selected to be in vacuum, as the solvation and ionization processes will be done later using GROMACS. The rest of the options are left to the default values and the input generation options are selected for GROMACS.

The tool then provides the required files for the simulation of clay, like the force field (.itp) and the molecule definition (.gro). For the porphyrins, the force fields and the topology files were created using **acpppe** by Sayan Maity.

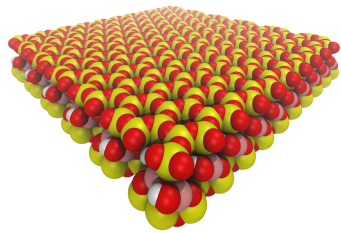


Figure 8: Montmorillonite surface

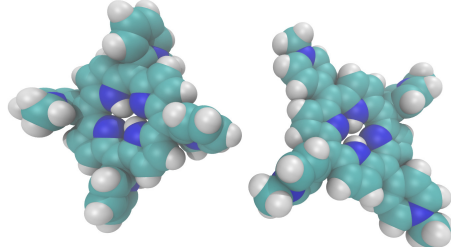


Figure 9: Porphyrin molecules

The first step to start preparing the simulation is merging the files, by making a single .gro file which includes the positions of the clay surface and the sixteen porphyrins. For this purpose, the position of the clay surface within the simulation box was first adjusted using the VMD software [10]. The clay surface was moved towards the edge of the simulation box to give more space for porphyrins to move. GROMACS was then used to position the porphyrins inside this simulation box by using the insert-molecules command from gmx. This GROMACS command allows for the selection of two .gro files to merge into one by also specifying the number of times it should be included. This way four m-TMPyP and twelve p-TMPyP molecules were added. The program places the molecules in a random position and with a random rotation inside the box, an example of this can be seen in fig 10. After the GROMACS file was ready with the positions of the molecules, the topology file (.top) provided by CHARMM-GUI was adjusted so that it included the newly added porphyrins and their force fields. The size of the unit cell was kept the same as the one specified in the CHARMM-GUI interface.

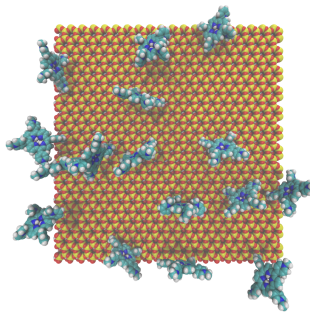


Figure 10: Clay/Porphyrin system

2.2 Solvation

After preparing the files, GROMACS could start being used to prepare the rest of the simulation. The first step in a standard MD simulation is to solvate the system, as the files mentioned previously still do not include any solvent and the molecules are in vacuum. For this the command **solvate** of GROMACS was used. The command used was **gmx solvate -cp InitialFixedPositions.gro -o solvated.gro -p topol.top**. This command takes the .gro file of the system and returns a file (solvated.gro) which consists of the system and the newly added molecules of water. The default algorithm for solvation was used (spc216.gro), and the model of water used in this simulation is TIP3.

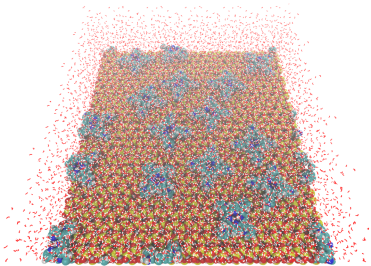


Figure 11: Solvated system

2.3 Ionization

After solvation, the issue of the system having a net charge must be addressed. The porphyrins have a positive charge, and the clay surface has a negative charge, which can be larger or smaller than the combined charge of the porphyrins. Therefore, the system as a whole may have a positive, neutral or negative net charge. Using the **genion** command from GROMACS chloride ions or sodium ions are added to make the net charge of the system zero. First the input files were prepared using the command **gmx grompp -f ionsmdp -c solvated.gro -r solvated.gro -p topol.top -o ions.tpr**, then these files were used to produce the GROMACS file with the ions using **gmx genion -s ions.tpr -o ionized.gro -p topol.top -pname NA -nname CL -neutral** and selecting option 6 (Solvent) when prompted to choose the residue to be replaced by ions.

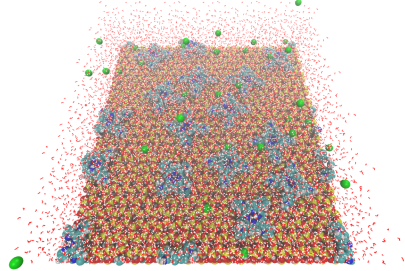


Figure 12: Ionized system

2.4 Energy Minimization

After ionization, all additions to the system have been made. However, it is still not ready for the simulation. First it has to go through energy minimization and NVT and NPT equilibration, which will ensure that the system is in a stable configuration before starting the production simulation. The process of energy minimization (EM) is used to relax the structure. The steps to perform EM are similar to the ones for ionization. First, the input files are generated, **gmx grompp -f step4.0_minimization.mdp -c ionized.gro -r ionized.gro -p topol.top -o em.tpr** and then the minimization is carried out by using **gmx mdrun -v -deffnm em**. The energy minimization was performed with a maximum of 50000 steps; however, the minimization stops when a certain requirement is met. After the minimization is performed, the potential energy of the system should be negative and be in the order of $10^5 - 10^6$. The effect of EM on the potential energy can be seen in fig 13.

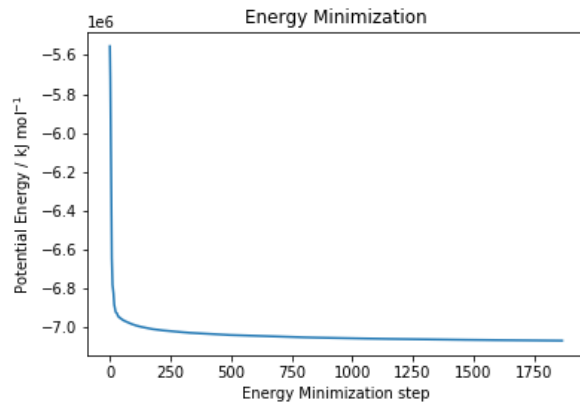


Figure 13: Potential Energy vs steps

2.5 NVT and NPT Equilibration

Now that we have a reasonable starting structure the next step is to equilibrate the system. The purpose of this equilibration is to bring everything to the same temperature and the same pressure and to equilibrate the solvent and ions around the other molecules [11]. For this, position restraints were used on the porphyrins and clay surface so that just water molecules and ions moved around. This equilibration is conducted in two phases, the first one is conducted under an NVT ensemble, i.e., keeping a constant number of particles, volume and temperature. The NVT equilibration was performed for 100 ps. The commands used were **gmx grompp -f nvtmdp -c em.gro -r em.gro -p topol.top -o nvt.tpr** to prepare the input, and **gmx mdrun -deffnm -v nvt** to run the equilibration itself. The NPT equilibration is performed afterwards, in which the pressure is now the parameter being kept constant. The NPT equilibration was also performed for 100 ps. The commands used were **gmx grompp -f nptmdp -c nvt.gro -r nvt.gro -t nvt.cpt -p topol.top -o npt.tpr** and **gmx mdrun -v -deffnm npt**. The change in temperature throughout the NVT equilibration can be seen in fig 14, where it can be noted that the temperature fluctuates. However, after some time it stays around the target value of 298.15 K. In the case of pressure for NPT equilibration, the standard deviation of the data is considerable. The pressure oscillates strongly into positive and negative pressures as seen in fig 15. However, when considering the standard deviation from the average (-11056 ± 87036 bar), it can be noticed that the target value (1.0 bar) is within the range covered by the standard deviation. From NPT equilibration one can also study the change of density throughout the process, shown in fig 16. The average value obtained is 1371 ± 97 kg m⁻³, which is slightly close to the density of water, as expected.

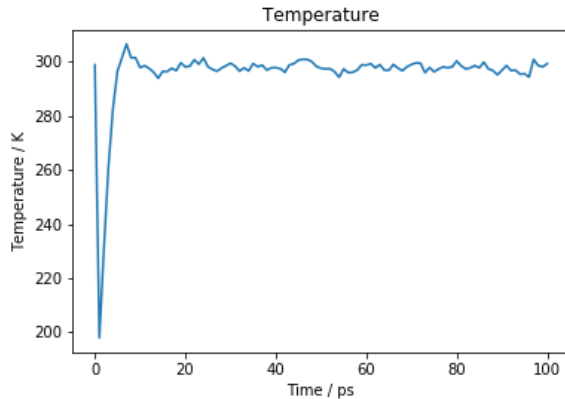


Figure 14: Temperature vs steps

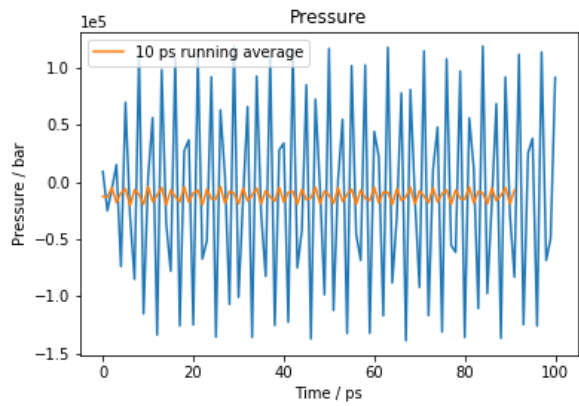


Figure 15: Pressure vs steps

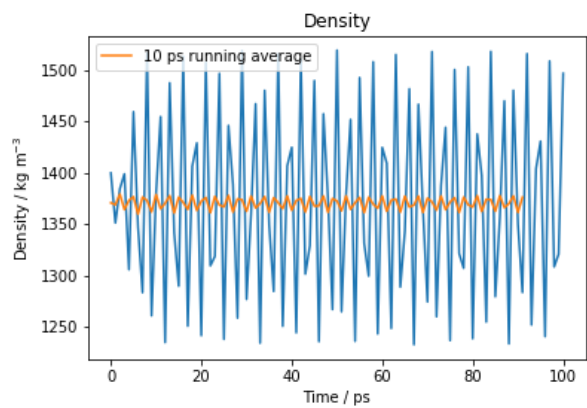


Figure 16: Density vs steps

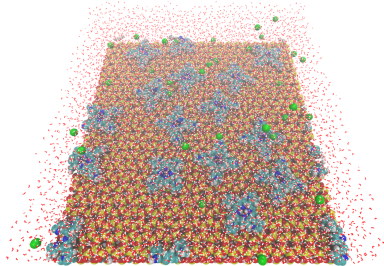


Figure 17: Equilibrated system

Now that the system has been minimized and equilibrated it is finally ready to run the production simulation. The simulations were performed for 30 ns, and two walls were used in the z axis in order to disable the periodicity of the simulation in the z axis. This allowed for having a smaller simulation box without having interference from periodic images, especially a periodic clay surface which could attract the porphyrins in the opposite direction. The commands used are similar to the ones discussed previously, **gmx grompp -f step5_productionmdp -c npt.gro -r npt.gro -t npt cpt -p topol.top -o md_0_1.tpr** to produce the binary input files, and **gmx mdrun -v -deffnm md_0_1** to run the simulation. After the simulation is finished it can now be visualized in VMD for further analysis by loading the molecules file **md_0_1.gro** and loading the trajectory file **md_0_1.xtc** into it.

2.6 Generation of Initial Configuration

Computer simulations of molecular systems face a great challenge. For a computer to generate data in time scales comparable to experiments performed in the laboratory it takes an unfeasible amount of time. For this reason, many times it is useful to start with a configuration which is believed to be close to the final convergence of the system.

This was the case for the performed simulations. The process described previously defines a standard MD simulation. However, knowing that the porphyrins would be attracted to the clay surface, an initial configuration was chosen such that the porphyrins were in direct contact with the surface. However, the molecules could not simply be dragged around, as it was still unknown what the distance between atoms should be so that the system is in a stable condition. For this reason, a short preliminary simulation was performed. The purpose of this simulation was to let the molecules interact merely through electrostatic interactions. This was done by running the simulation without water molecules nor ions. For this, from the previously described steps, the topology preparation was done. Then, solvation and ionization were skipped, and then the following steps were performed normally. The vacuum simulations were performed for a

maximum of 5 ns, however, the porphyrins got to stable positions after a few picoseconds. The changes that this had during the process can be seen in fig 18. For energy minimization progress was similar, with potential energy decreasing to a negative value in the order of 10_6 . However, this was not the case for the NVT and NPT parameters. Temperature is now further away from the target value of 298.15 K. In the case of pressure, the oscillation between negative and positive values was slower, which means that the standard deviation increased, in this case being an order of magnitude larger than the average (1693 ± 55743 bar). The density also suffered changes, it decreased from the values previously obtained. All these changes were expected, as a vacuum simulation is not standard, however it served the purpose of getting a better initial configuration as shown in fig 19. VMD was then used to extract the last frame of the simulation and use it as initial configuration for the 30 ns simulation.

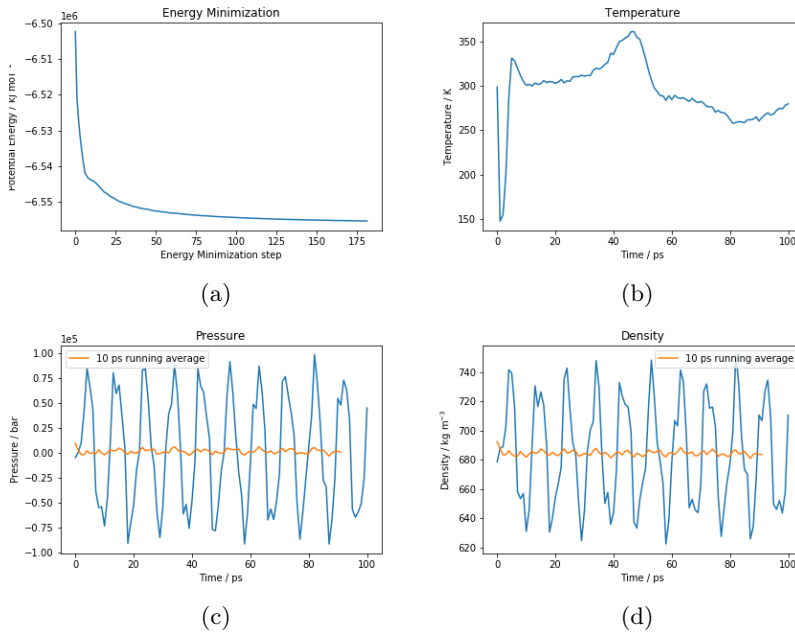


Figure 18: Graphs from procedure of vacuum simulation

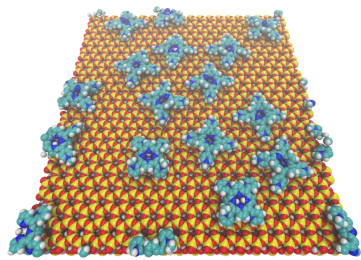


Figure 19: Initial configuration generated by vacuum simulation

3 Results and Discussion

In this thesis the adsorption of porphyrin molecules on a montmorillonite surface was studied by running simulations following the steps described in the previous section. The adsorption was analyzed in configurations with different x values to produce surfaces with different charges. Then, the adsorption was compared to the inter-charge distance difference between porphyrins and the clay surface.

The simulations that are analyzed in this section of the thesis were performed for 30 ns. Four m-TMPyP and twelve p-TMPyP molecules were used, resulting in a 1:3 ratio of m-TMPyP and p-TMPyP porphyrins. This ratio was utilized as it was proved in previous literature that it can produce the best energy transfer efficiencies [7]. The data produced by GROMACS from the simulations was visually analyzed by using VMD. Then, for graph production and further analysis, the MDanalysis [12] library was used in Python.

3.1 Determination of Inter-charge Distances

After loading the coordinate and topology files into a Jupyter notebook by using MDanalysis, the inter-charge distances were determined for the porphyrins and the clay surface. For the clay surface, it meant measuring the distance between Mg atoms in the middle layer of the surface. However, the Mg atoms in the surface given by CHARMM-GUI are randomly distributed. This means that the inter-charge distance cannot simply be obtained by measuring the distances between Mg atoms, as they vary within the surface. For this reason, a different approach had to be utilized. As the size of the system being simulated was small compared to what it could be in an experimental situation in the laboratory, some assumptions had to be made. As the Mg atoms are randomly placed, they are not positioned regularly on the surface, but in a larger surface it could be assumed that the average inter-charge distance would approach that one of an equidistant distribution along the surface. Then, the inter-charge distance could be calculated by considering the Mg atoms to be equally distributed along the surface. With this assumption, the total area of the surface could be calculated ($100 \text{ \AA} \times 100 \text{ \AA}$) and then divided by the number of Mg atoms, which represents the area per atom. Now that the area per atom has been calculated the distance between atoms can be calculated by taking the square root of the area per atom. This way the inter-charge distances were calculated for the six simulations with different x values, shown in table 1. In the case of porphyrins this meant simply measuring the distance between the N atoms at the extremes of the molecule. For the m-TMPyP molecules the distance was measured to be 8.99 \AA , and for p-TMPyP, the distance was 11.36 \AA .

The calculated inter-charge distances in the clay surface are comparable to the range of distances calculated in literature ($8 - 19 \text{ \AA}$) [13]. The measured distances for the porphyrins are comparable to the ones found in fig 5 [7].

x value	MG atoms	Inter-charge distance / Å
0.06	28	18.90
0.08	38	16.22
0.1333	64	12.50
0.20	96	10.21
0.45	216	6.80
0.94	452	4.70

Table 1: Inter-charge distances for surfaces with different x values

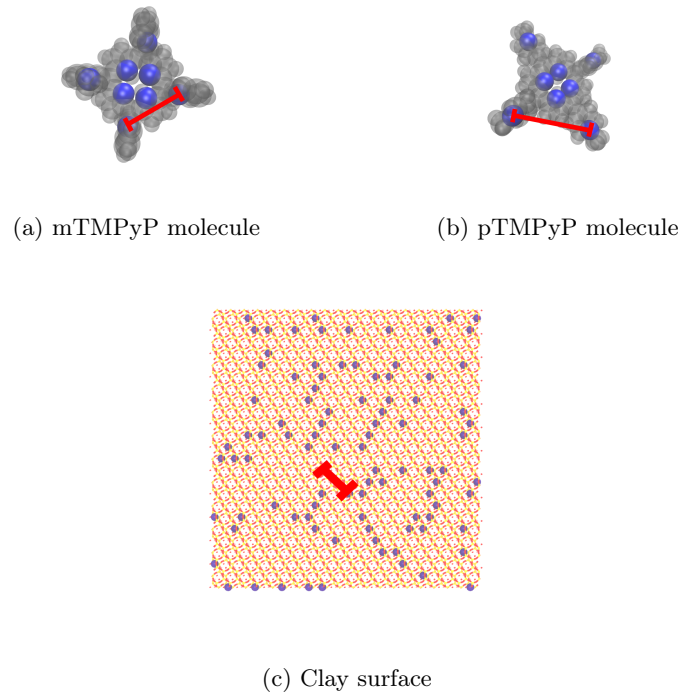


Figure 20: Inter-charge distances in porphyrins and clay

3.2 Porphyrin Movement through the Simulation

From the trajectory file imported into Python the individual trajectories of each porphyrin can be extracted. The information of each porphyrin was obtained for all the individual frames, and then the center of mass was obtained using a function from MDAnalysis and stored in a variable. The moving average the height of each of the porphyrins was plotted using a window size of 100 steps for the average. The plots were realized for each of the systems with different x values, and height average of all the porphyrins throughout the simulation was

also plotted as a horizontal dashed line. These graphs are shown in fig 21.

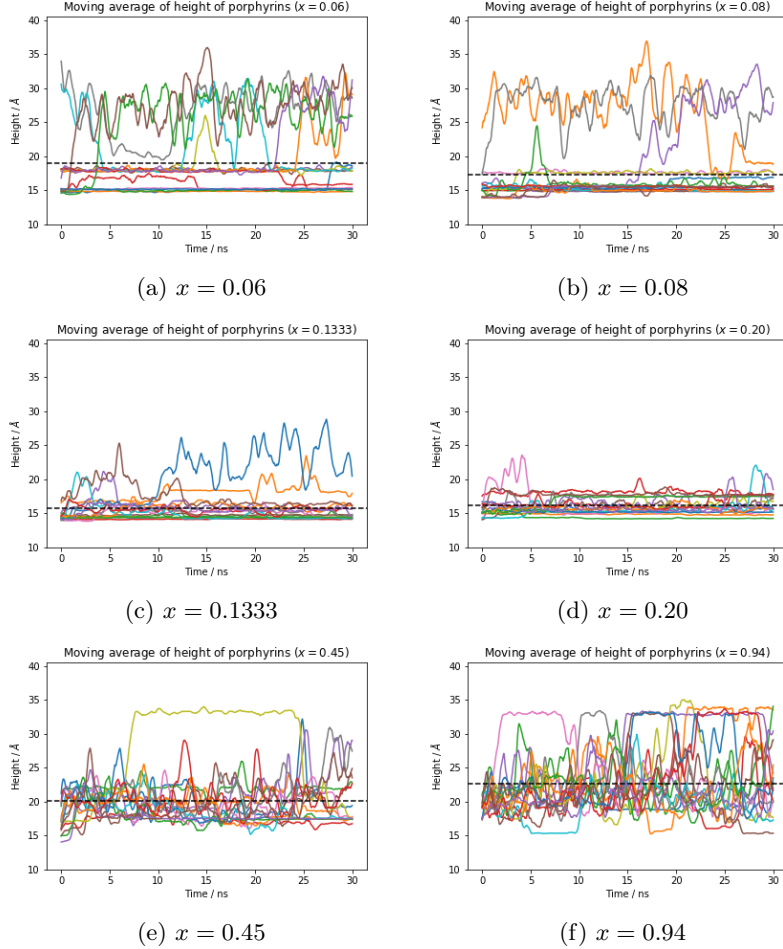


Figure 21: Porphyrin movement throughout the simulation

As it can be seen in the different graphs, the minimum distance is close to 13 Å, this is because the clay surface is at that distance, and the porphyrins cannot simply go through it. The maximum height allowed by the simulation box is of 40.60 Å. It can be noted that for x values of 0.08, 0.1333 and 0.20 the distribution of the porphyrins is quite close to the surface, apart from a couple of porphyrins. For these graphs there is a group of straight lines, which means that the porphyrins did not move significantly throughout the simulation, an indication that these porphyrins were adsorbed. It can also be noted for example in $x = 0.20$, that there may be straight lines at two different heights. After visually inspecting the trajectories using VMD, it can be inferred that the higher group of straight lines is caused by porphyrins that bend after adsorption,

as the height is measured from the center of mass, and while being in contact, other parts of the molecules may be bent upwards. However, for x values of 0.45 and 0.94, a more erratic behavior from the porphyrins can be noted. This seems to be counterintuitive, as the surfaces have a stronger electric charge, meaning that the attraction between porphyrins and surface should be stronger. Nevertheless, after visually inspecting the trajectories of the porphyrins, it was noted that the neutralizing ions have a strong effect on the adsorption of the molecules. The neutralizing ions, in this case chloride ion and sodium ion, have a higher charge density than the porphyrins. This means that the ions will have a stronger interaction, while having a smaller volume, which allows them to move through the water molecules more easily than the porphyrins. Once the ions reach the surface, they get embedded into it. As the charge of the ions has the same sign as the one of the porphyrins (for $x > 0.1333$), they interfere with the adsorption of the porphyrins by pushing them away from the surface. This behavior can be seen in fig 22f.

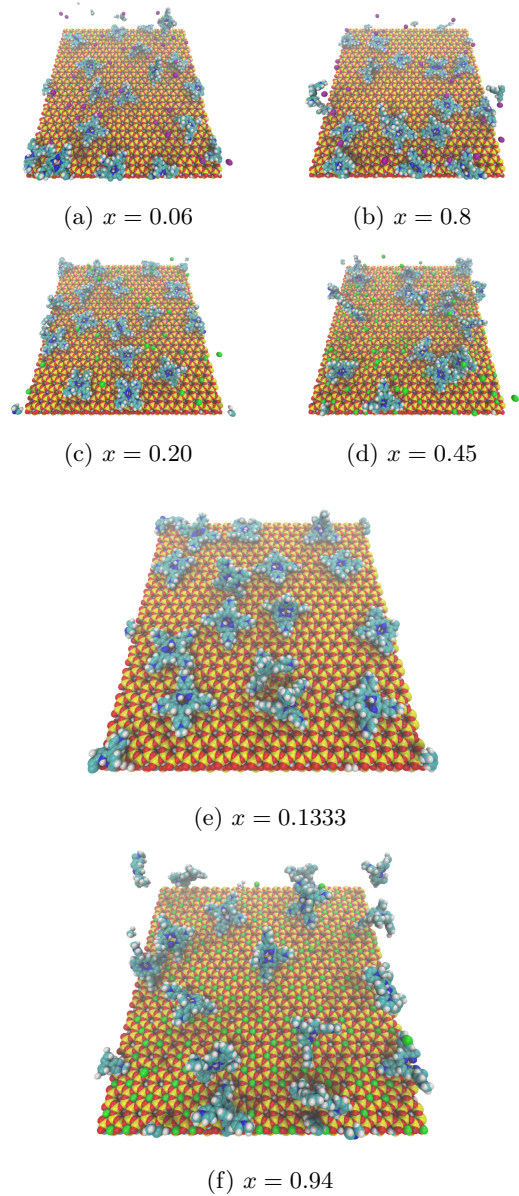


Figure 22: Final configurations for the different systems. The most interesting systems are enlarged. In fig (e) it can be noticed that there are no neutralizing ions that interfere with the adsorption of porphyrins. In fig (f) it is noted that the ions are adsorbed by the surface and impede the adsorption of the porphyrins

3.3 Assessing the Adsorption Percentage

Now that the movement of the porphyrins has been qualitatively analyzed, it would prove useful to classify further and determine the number of porphyrins adsorbed by the surface. For this, the height information of the porphyrins was used. However, in this case it was considered just for the second half of the simulation, as it is assumed that the porphyrins need some simulation time to find their stable positions. For this reason, the height data was taken from 15 ns to 30 ns. With the data prepared, now the average and standard deviation of the trajectory of each porphyrin has to be analyzed to decide if the porphyrin is adsorbed or not. In order to classify the porphyrins as adsorbed or not, some limiting parameters had to be found. This was done visually by using a violin plot and also with support from the trajectory visualization in VMD. After analyzing the plots and trajectories, it was decided that a porphyrin could be considered to be adsorbed if the mean of its height is lower than 19.5 Å and the standard deviation is lower than 1.2 Å. Python was used once again to prepare the violin plots of the porphyrin trajectories, which are shown in fig 23. In a violin plot, the median, interquartile range and density distribution are displayed. The white dot in the middle represents the median height. The thicker bar represents the interquartile range. And the kernel on each side of the gray line displays the distribution of the data, if the violin is wider, it means that the data is concentrated around the median and the standard deviation is small [14]. This type of plot was made for all the different simulations. The height of the violins was also considered, as it shows the span of the molecule during the simulation. A tall but thin violin means that the molecule had a lot of movement, and hence, did not stick to the surface. The number of porphyrins adsorbed by each surface can be seen in table 2.

The number of adsorbed porphyrins confirms that adsorption does not solely depend on strength of Coulomb attraction. The medium in which the molecules are placed also interferes with their adsorption. In these graphs it can be noted that for $x = 0.08$, even though it provides the weakest attraction between porphyrin and clay, the distinction between adsorbed and not adsorbed porphyrins is clearer. Even though not all the porphyrins were adsorbed, the ones that were adsorbed have a denser distribution, while the ones that were not adsorbed were displaced through a large range of heights, clearly showing that they were not adsorbed.

3.4 Intermolecular Distance of Porphyrins

Now that the number of adsorbed porphyrins has been established, the distance between the porphyrins that were adsorbed might be of interest. By applying similar assumptions to the ones in section **Determination of Inter-charge Distances** the intermolecular distance can now be calculated. The method of calculating the distances was the same as the one described previously but using now just the number of adsorbed porphyrins. The resulting distances can be seen in table 2.

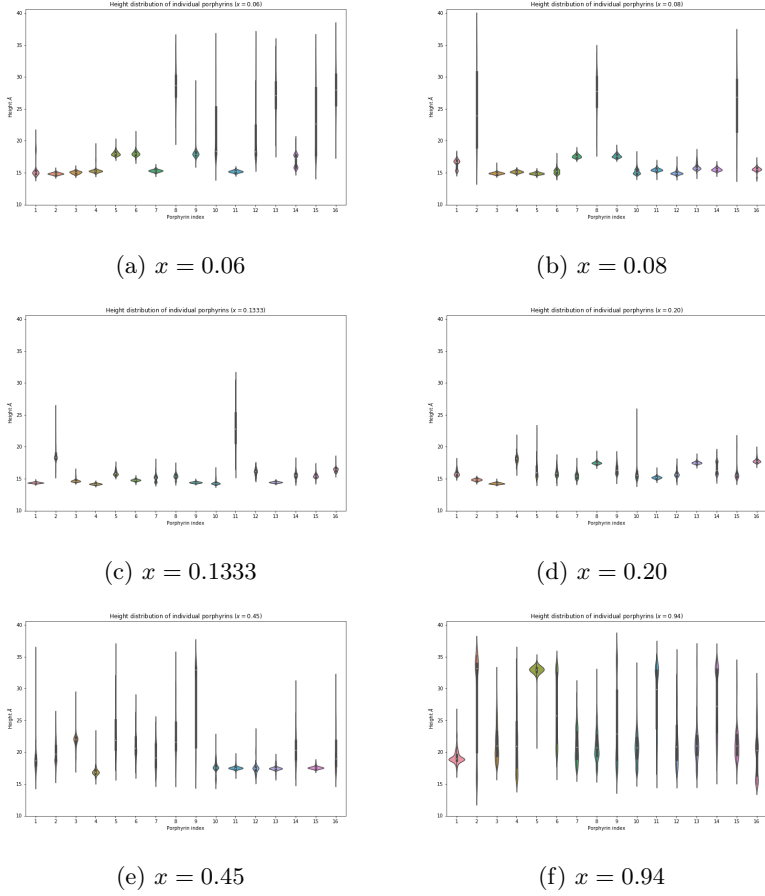


Figure 23: Violin plots for the different systems

x value	Adsorbed porphyrins	Intermolecular distance / Å
0.06	8	35.36
0.08	13	27.74
0.1333	14	26.73
0.20	14	26.73
0.45	6	40.82
0.94	1	100.00

Table 2: Intermolecular distance

The inter-charge distance can be important for the light harvesting capabilities of the porphyrin/clay complex. Here we can see an evident relation between the x value and the intermolecular distance. This is useful, as it means that

as long as the charge distribution can be modified on the surface the adsorption structure can also be modified. These values are somewhat close to the intermolecular distance proposed by the literature [15].



Figure 24: Distribution of porphyrins and Mg atoms

3.5 Relationship between Inter-charge Distances

Another relationship that might be of interest is the connection between the inter-charge distances of porphyrins and clay and the adsorption of the later on the former. This inspired by the paper on size-matching effect [15] where it is argued that the agreement of the inter-charge distances in porphyrins and clay have direct influence on the adsorption percentage. The difference in the inter-charge distances is also connected to the charge density of both porphyrins and clay. The way this inter-charge distance difference is determined is shown in fig 25. The resulting graph obtained in this study is shown in fig 26.

The relationship between inter-charge distance difference and the adsorption of porphyrins is therefore supported by the graph previously shown. The obtained graph closely resembles the distribution of the experimental relationship from [15] (shown as red crosses). However, the graph determined through MD simulation has higher adsorption percentage for positive values, which means that the charge density of the surfaces is smaller than the total charge of the porphyrins. This is due to the interaction of the neutralizing ions, which in the case of being chloride ions have same charge than the surface, and therefore move away from it, leaving more space for the porphyrins.

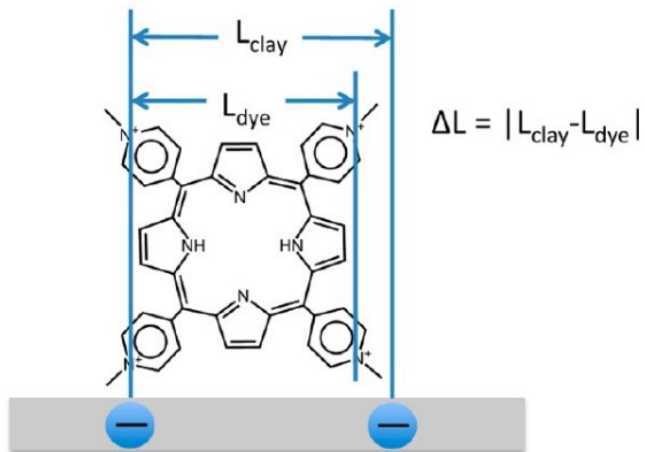


Figure 25: Calculation of inter-charge distance difference. Retrieved from [15]

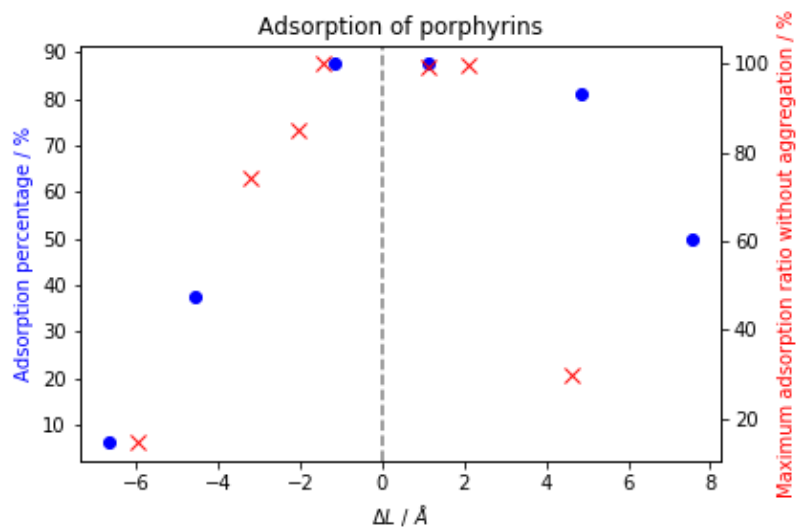


Figure 26: Adsorption of porphyrins as a function of inter-charge distance difference. The red crosses show the experimental data obtained from [15].

4 Conclusion and Outlook

Several simulations were performed with the objective of reproducing and analyzing the adsorption of porphyrin molecules on a montmorillonite surface. After analyzing the simulations, it was evident that the main influence in adsorption is given by the electrostatic forces between charges. However, it was also noted that there are other influences in porphyrin adsorption. It was found that the movement of water molecules and neutralizing ions also influenced molecule adsorption significantly, in some cases cancelling out the effect of attraction between porphyrins and the clay surface. This can be seen specially for systems with high charge difference between the porphyrins and the surface, in which many neutralizing ions must be added. These ions produce the counterintuitive result of having the smallest percentage of adsorption when the charge difference between porphyrins and surface is the largest.

Throughout the different simulations porphyrins were able to attach to the clay surface to some degree, producing variations of the desired system in which porphyrins adsorb into the clay surface. No adsorption of 100% was achieved, however, this could be due to choosing an arbitrary number of porphyrins for the surface size. The maximum number of adsorbed porphyrins was 14 out of 16, which can mean that the surface saturates at 14 molecules, and in order to adsorb all the 16 molecules a slightly larger surface would be needed. There is also the possibility, however, that because of the limitations that computer simulations have, the actual experimental conditions could not be directly reproduced. In the experimental procedure solutions with all the components are mixed and vigorously stirred, after an hour, the adsorption of porphyrins on the surface is finished [7]. In the scope of this thesis, it was just possible to simulate small systems of 16 molecules for a time of 30 ns, which is extremely different to the experimental time. Also, the exact conditions of a stirring movement cannot be imitated, it is dealt with by simply adding random velocities to the particles using the temperature as reference. Despite these limitations, a similar behavior to the experiment was observed in the simulations, and so the data can be useful to approximate what is happening in the laboratory experiment.

It can be said that this numerical experiment was successful. The results obtained compare well to experimental results from other sources. The relationship between inter-charge distance and porphyrin adsorption is specially interesting. These results prove numerically the **size matching** effect described in the paper by Shinsuke Takagi, et.al [15]. However, it is also noted that the adsorption for positive ΔL values is higher. From visual inspection of the simulation trajectories, it can be inferred that the effect of neutralizing ions seems to be higher when the charge of the ions has the same sign as the surface.

The results obtained in this thesis help to further understand the dynamics behind dye adsorption on clay surfaces. Having a computer simulation of the adsorption process allows to study the molecules more in detail and could be useful for identifying events that can affect the evolution of the macroscopic system. The data generated by the MD simulation can also now be used to run other type of simulations, with a more accurate description of the porphyrin/clay

system than if the positions of molecules were just assumed. The trajectory files can be used, for example, to perform quantum dynamics simulations in order to understand better the energy transfer in the system, and possibly obtaining maximum efficiency values.

5 Acknowledgements

First, I would like to thank my supervisors, Prof. Ulrich Kleinekathöfer and Sayan Maity. Without their assistance I would not have been able to understand the simulation system and obtain the desired results. I would also like to thank them for their availability and patience in helping me face technical problems along the way. The discussions I had with them during the process were always interesting and fruitful. I would also like to thank all my professors. Without them I would not be able to understand the topics I can understand today, and I would not have the passion for science required to enjoy it. I would also like to thank my family, who have always been there providing emotional and financial support. I would like to thank my dad for the opportunity he gifted me of undertaking my higher education abroad, as I have always dreamt about when I was a kid. I would also like to thank him for cultivating scientific critical thinking in me, which made me who I am today. I want to thank my sisters for always being there for me and being my closest friends. I want to thank my friends who make my life better and motivate me to keep moving forward. And lastly, I would like to thank every person that I have met throughout my life that has helped me guide my path and become who I am today.

6 References

- [1] Michael P. Allen. “Introduction to Molecular Dynamics Simulation”. In: *NIC Series Volume 23 : Computational Soft Matter: From Synthetic Polymers to Proteins, Lecture Notes*. Vol. 23. NIC series. Jülich: John von Neumann Institute for Computing, 2004, pp. 1–28. URL: <https://juser.fz-juelich.de/record/152581>.
- [2] P. Schuster. “G. C. Maitland, M. Rigby, E. B. Smith, W. A. Wakeham: Intermolecular Forces – Their Origin and Determination, Clarendon Press, Oxford 1981. 616 Seiten, Preis \$ 39.50”. In: *Berichte der Bunsengesellschaft für physikalische Chemie* 87.3 (1983), pp. 291–292. DOI: <https://doi.org/10.1002/bbpc.19830870335>.
- [3] GROMACS development team. *Reference Manual: GROMACS 2020.6*. URL: <https://manual.gromacs.org/documentation/2020-current/reference-manual/index.html>.
- [4] Michael Grätzel. “Dye-sensitized solar cells”. In: *Journal of Photochemistry and Photobiology C: Photochemistry Reviews* 4.2 (2003), pp. 145–153. DOI: [https://doi.org/10.1016/S1389-5567\(03\)00026-1](https://doi.org/10.1016/S1389-5567(03)00026-1).
- [5] Tomohiro Higashino and Hiroshi Imahori. “Porphyrins as excellent dyes for dye-sensitized solar cells: recent developments and insights”. In: *Dalton Transactions* 44 (2 2015), pp. 448–463. URL: <http://dx.doi.org/10.1039/C4DT02756F>.
- [6] Matthew J. Griffith et al. “Porphyrins for dye-sensitised solar cells: new insights into efficiency-determining electron transfer steps”. In: *Chemical Communications* 48 (35 2012), pp. 4145–4162. URL: <http://dx.doi.org/10.1039/C2CC30677H>.
- [7] Yohei Ishida, Tetsuya Shimada, Dai Masui, Hiroshi Tachibana, Haruo Inoue, and Shinsuke Takagi. “Efficient Excited Energy Transfer Reaction in Clay/Porphyrin Complex toward an Artificial Light-Harvesting System”. In: *Journal of the American Chemical Society* 133.36 (2011), pp. 14280–14286. DOI: <10.1021/ja204425u>. URL: <https://doi.org/10.1021/ja204425u>.
- [8] Wenyuan Sun, Hongbo Zeng, and Tian Tang. “Synergetic adsorption of polymers on montmorillonite: Insights from molecular dynamics simulations”. In: *Applied Clay Science* 193 (2020), p. 105654. ISSN: 0169-1317. DOI: <https://doi.org/10.1016/j.clay.2020.105654>.
- [9] Lehigh University. *CHARMM-GUI: Effective Simulation Input Generator and More*. URL: <https://charmm-gui.org/>.
- [10] Beckman Institute for Advanced Science, Technology, National Institutes of Health, National Science Foundation, Computer Science Physics, and Biophysics at University of Illinois at Urbana-Champaign. *VMD (Visual Molecular Dynamics)*. URL: <https://www.ks.uiuc.edu/Research/vmd/>.

- [11] Ph.D. Justin A. Lemkul. *Gromacs Tutorial: Lysozyme in Water*. URL: <http://www.mdtutorials.com/gmx/lysozyme/index.html>.
- [12] MDAnalysis core developers. *About MDAnalysis*. URL: <https://www.mdanalysis.org/about/>.
- [13] Tsuyoshi Egawa et al. “Novel Methodology To Control the Adsorption Structure of Cationic Porphyrins on the Clay Surface Using the “Size-Matching Rule””. In: *Langmuir* 27.17 (2011), pp. 10722–10729. URL: <https://doi.org/10.1021/la202231k>.
- [14] Joel Carron. *Violin Plots 101: Visualizing Distribution and Probability Density*. URL: <https://mode.com/blog/violin-plot-examples/>.
- [15] Shinsuke Takagi, Tetsuya Shimada, Yohei Ishida, Takuya Fujimura, Dai Masui, Hiroshi Tachibana, Miharu Eguchi, and Haruo Inoue. “Size-Matching Effect on Inorganic Nanosheets: Control of Distance, Alignment, and Orientation of Molecular Adsorption as a Bottom-Up Methodology for Nanomaterials”. In: *Langmuir* 29.7 (2013), pp. 2108–2119. URL: <https://doi.org/10.1021/la3034808>.

Statutory Declaration

Family Name, Given/First Name	Salazar Letona, Carlos Rafael
Matriculation number	30002031
What kind of thesis are you submitting: Bachelor-, Master- or PhD-Thesis	Bachelor Thesis

English: Declaration of Authorship

I hereby declare that the thesis submitted was created and written solely by myself without any external support. Any sources, direct or indirect, are marked as such. I am aware of the fact that the contents of the thesis in digital form may be revised with regard to usage of unauthorized aid as well as whether the whole or parts of it may be identified as plagiarism. I do agree my work to be entered into a database for it to be compared with existing sources, where it will remain in order to enable further comparisons with future theses. This does not grant any rights of reproduction and usage, however.

This document was neither presented to any other examination board nor has it been published.

German: Erklärung der Autorenschaft (Urheberschaft)

Ich erkläre hiermit, dass die vorliegende Arbeit ohne fremde Hilfe ausschließlich von mir erstellt und geschrieben worden ist. Jedwede verwendeten Quellen, direkter oder indirekter Art, sind als solche kenntlich gemacht worden. Mir ist die Tatsache bewusst, dass der Inhalt der Thesis in digitaler Form geprüft werden kann im Hinblick darauf, ob es sich ganz oder in Teilen um ein Plagiat handelt. Ich bin damit einverstanden, dass meine Arbeit in einer Datenbank eingegeben werden kann, um mit bereits bestehenden Quellen verglichen zu werden und dort auch verbleibt, um mit zukünftigen Arbeiten verglichen werden zu können. Dies berechtigt jedoch nicht zur Verwendung oder Vervielfältigung.

Diese Arbeit wurde noch keiner anderen Prüfungsbehörde vorgelegt noch wurde sie bisher veröffentlicht.

17.05.2021 *Carlos*
.....
Date, Signature